

# Determination of the Molecular Conformation of Melanostatin Using $^{13}\text{C}$ , $^{15}\text{N}$ -REDOR NMR Spectroscopy

Joel R. Garbow\* and Charles A. McWherter

Contribution from Monsanto Corporate Research, Monsanto Company, 700 Chesterfield Parkway North, St. Louis, Missouri 63198. Received June 1, 1992

**Abstract:** Results of a  $^{13}\text{C}$ ,  $^{15}\text{N}$ -rotational-echo double-resonance (REDOR) NMR study of the neurohormonal tripeptide melanostatin (Pro-Leu-Gly-NH<sub>2</sub>) are reported. The REDOR experiment permits through-space carbon-nitrogen distances to be accurately measured in solid samples. REDOR distances spanning the range 2.4 Å to 4.9 Å are measured for a series of selectively  $^{13}\text{C}$ ,  $^{15}\text{N}$ -enriched melanostatins and are in good agreement with those reported in the X-ray structure. The REDOR distances provide effective constraints on the values of the dihedral angles  $\phi_{\text{Leu}}$ ,  $\psi_{\text{Leu}}$ , and  $\phi_{\text{Gly}}$  in the tripeptide. Together with conservative energetic considerations, the REDOR-measured distances determine a family of backbone structures for the tripeptide.  $\phi_{\text{Leu}}$  is limited to the range  $-70^\circ$  to  $+20^\circ$ ,  $\psi_{\text{Leu}}$  from  $130^\circ$  to  $145^\circ$ , and  $\phi_{\text{Gly}}$  from  $-5^\circ$  to  $+65^\circ$ . For a 14-atom backbone fragment, the pairwise, minimum root-mean-square deviation (RMSD) between the family of REDOR structures and the X-ray conformation is  $0.437 \pm 0.224$  Å (avg  $\pm$  std dev). Based upon this work, a general strategy for selecting labeling sites in peptides and proteins to determine their backbone conformations is described.

## Introduction

The classic approach to drug discovery correlates molecular properties with biological activity for a series of related molecules. Extensions of this approach attempt to derive theoretical models describing the docking geometry of ligands bound to their macromolecular receptors. By providing structural information at atomic resolution, X-ray crystallography studies of ligand-receptor complexes can contribute significantly to this approach. Unfortunately, many systems are not amenable to X-ray diffraction studies because of the difficulty in obtaining suitable crystals.<sup>1</sup> Recently, high-resolution NMR experiments have been used to determine the conformation of isotopically-enriched cyclosporin A complexed with the enzyme cyclophilin.<sup>2</sup> The efficacy of these and other solution NMR methods can be limited by both the molecular size and solubility of the receptor.<sup>3</sup> The recent development of  $^{13}\text{C}$ ,  $^{15}\text{N}$ -rotational-echo double-resonance (REDOR) NMR spectroscopy<sup>4-7</sup> for determining carbon-to-nitrogen distances in solids is directly applicable to the problem of determining bound-ligand conformations without limitations imposed by crystallization, molecular weight, or solubility.

We report here our efforts to define the methods and requirements for constructing structural models from REDOR data.<sup>8</sup> As a model system, we use the tripeptide melanostatin (Pro-Leu-Gly-NH<sub>2</sub>), a neurohormone responsible for modulating dopamine receptors in the central nervous system<sup>9</sup> which may also inhibit the release of melanin-stimulating hormone.<sup>10</sup> We have prepared a series of selectively  $^{13}\text{C}$ ,  $^{15}\text{N}$ -labeled melanostatins for study by  $^{13}\text{C}$ -detected REDOR. From the REDOR data,  $^{13}\text{C}$ - $^{15}\text{N}$  dipolar coupling constants are determined, allowing the distances between the  $^{13}\text{C}$ - and  $^{15}\text{N}$ -labeled sites to be calculated. A comparison is made between REDOR-determined distances and those calculated from the type II bend structure determined by X-ray crystallography.<sup>11,12</sup> Our results show how the REDOR distances effectively constrain the backbone dihedral angles of melanostatin, thereby providing a direct determination of its solid-state conformation. Finally, on the basis of the tripeptide work, we describe a general strategy for selecting  $^{13}\text{C}$ ,  $^{15}\text{N}$  labeling sites for the effective mapping of the backbone conformations of peptides and proteins.

## Experimental Section

**Materials.** N-t-Boc amino acids were obtained from Advanced Chemtech (Louisville, KY).  $^{13}\text{C}$  and  $^{15}\text{N}$  selectively enriched amino acids were obtained from either MSD Isotopes ([1- $^{13}\text{C}$ ]Pro, [1- $^{13}\text{C}$ ,  $^{15}\text{N}$ ]Leu, and [ $^{15}\text{N}$ ]Gly; Montreal, Quebec, Canada) or Sigma Chemical Co. ([2- $^{13}\text{C}$ ]Gly and [ $^{15}\text{N}$ ]Leu; St. Louis, MO); Boc-[1- $^{13}\text{C}$ ]Gly was obtained from MSD Isotopes. All Pro- and Leu-containing compounds used in

this study were of the L configuration. Di-*tert*-butyl pyrocarbonate was obtained from Sigma and MBHA resin was purchased from Fluka (Ronkonkoma, NY).

**Synthesis of  $^{13}\text{C}$ - and  $^{15}\text{N}$ -Enriched N-t-Boc Amino Acids.** The isotopically enriched amino acids were protected prior to use in solid-phase peptide synthesis using di-*tert*-butyl pyrocarbonate as described by Bodansky.<sup>13</sup> Boc-[1- $^{13}\text{C}$ ]Pro, Boc-[2- $^{13}\text{C}$ ]Gly, and Boc-[ $^{15}\text{N}$ ]Gly were crystallized on ice from ethyl acetate by addition of cold hexanes. Crystals were collected by vacuum filtration and dried overnight in vacuo over P<sub>2</sub>O<sub>5</sub>. Boc-[1- $^{13}\text{C}$ ,  $^{15}\text{N}$ ]Leu and Boc-[ $^{15}\text{N}$ ]Leu were crystallized on ice from EtOH by addition of ice cold H<sub>2</sub>O. The crystals were collected by vacuum filtration, air-dried, and stored desiccated until needed. The Boc-protected, heavy-atom amino acids were characterized by TLC, FAB mass spectrometry, 300-MHz <sup>1</sup>H NMR, and, for the  $^{13}\text{C}$ -labeled compounds, 75-MHz  $^{13}\text{C}$  NMR. All of the analytical data were consistent with the expected products.

**Melanostatin Synthesis.** All of the labeled melanostatins were prepared by manual stepwise synthesis using 0.5 mmol of MBHA resin (1-1.2 mequiv of NH<sub>2</sub>/g), essentially as described by Stewart and Young.<sup>14</sup> Couplings used equimolar amounts of Boc-protected amino acid and diisopropylcarbodiimide in CH<sub>2</sub>Cl<sub>2</sub>. The natural-abundance Boc-protected amino acids were coupled at 3-fold molar excesses over the resin substitution, and labeled compounds were used in 1.5- to 2-fold

(1) Blundell, T. L.; Johnson, L. N. *Protein Crystallography*; Academic Press: New York, 1976.

(2) (a) Weber, C.; Wider, G.; Von Freyburg, R.; Traber, R.; Braun, W.; Widmer, H.; Wuthrich, K. *Biochemistry* 1991, 30, 6563. (b) Fesik, S. W.; Gampe, R. T., Jr.; Eaton, H. L.; Gemmecker, G.; Olejniczak, E. T.; Neri, P.; Holzman, T. F.; Egan, D. A.; Edalji, R.; Simmer, R.; Helfrich, R.; Hochlowski, J.; Jackson, M. *Biochemistry* 1991, 30, 6574.

(3) Fesik, S. W. In *Computer-Aided Drug Design*; Perun, T. J., Propst, C. L., Eds.; Marcel-Dekker: New York, 1989; Chapter 5.

(4) Gullion, T.; Schaefer, J. *J. Magn. Reson.* 1989, 81, 196.

(5) Gullion, T.; Schaefer, J. *Adv. Magn. Reson.* 1989, 13, 55.

(6) Marshall, G. R.; Beusen, D. D.; Kociolek, K.; Redlinski, A. S.; Leplawy, M. T.; Pan, Y.; Schaefer, J. *J. Am. Chem. Soc.* 1990, 112, 963.

(7) Pan, Y.; Gullion, T.; Schaefer, J. *J. Magn. Reson.* 1990, 90, 330.

(8) Portions of this work were presented previously at the IUPAB Satellite Symposium, "Expanding Frontiers in Polypeptide and Protein Structural Research", Whistler, British Columbia, Canada, July 23-27, 1990, and in the proceedings thereof: Garbow, J. R.; McWherter, C. A. In *Proteins: Structure, Function, Dynamics*; Renugopalakrishnan, V.; Carey, P. R., Smith, I. C. P., Huang, S.-G., Storer, A. C., Eds.; ESCOM: Leiden, 1991; pp 74-78.

(9) Mishra, R. K.; Chiu, S.; Chiu, P.; Mishra, C. P. *Methods Find. Exp. Clin. Pharmacol.* 1983, 5, 203.

(10) Celis, M. E.; Taleisnik, S.; Walter, R. *Proc. Natl. Acad. Sci. U.S.A.* 1971, 68, 1428.

(11) Reed, L. L.; Johnson, P. L. *J. Am. Chem. Soc.* 1973, 95, 7523.

(12) McWherter, C. A.; Garbow, J. R.; Shieh, H.-S.; Chiang, M. Unpublished results.

(13) Bodansky, M.; Bodansky, A. *The Practice of Peptide Synthesis*; Springer-Verlag: New York, 1984; p 199.

(14) Stewart, J. M.; Young, J. D. *Solid Phase Peptide Synthesis*, 2nd ed.; Pierce Chemical Co.: Rockford, IL, 1984.

\* Author to whom correspondence should be addressed.

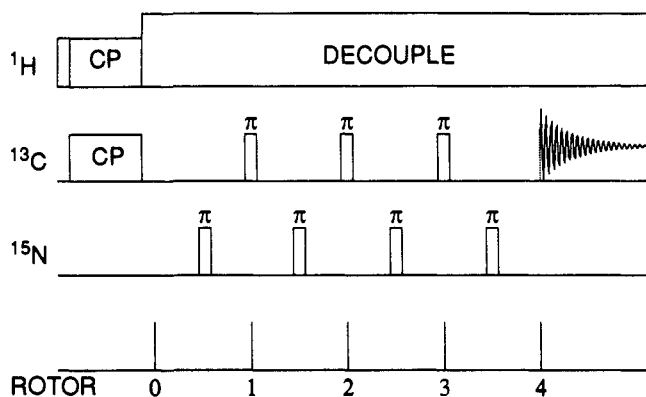


**Figure 1.** Pulse sequence for  $^{13}\text{C}$ -observed REDOR NMR. This sequence differs from the original REDOR pulse sequence<sup>4</sup> in that  $\pi$  pulses alternate between  $^{13}\text{C}$  and  $^{15}\text{N}$  rf channels. Applying one  $^{13}\text{C}$   $\pi$  pulse per rotor period helps to enhance sensitivity by reducing the loss of rotational-echo intensity as the total number of rotor periods,  $N_C$ , increases.<sup>18</sup> On alternate scans of the REDOR experiment, the  $^{15}\text{N}$   $\pi$  pulses are either applied or omitted. This figure illustrates the REDOR pulse sequence with four rotor periods of  $^{13}\text{C}$ - $^{15}\text{N}$  dipolar-coupling evolution ( $N_C = 4$ ).  $N_C$  can be increased (in increments of 2) by adding rotor periods and pairs of  $^{13}\text{C}$  and  $^{15}\text{N}$   $\pi$  pulses between the end of the cross-polarization preparation and the start of data acquisition.

excess. The coupling reaction was monitored for completion using the ninhydrin test for free amines; when necessary, the coupling was repeated. After coupling of the terminal proline was complete, the Boc group was removed by treating with 50% TFA in  $\text{CH}_2\text{Cl}_2$  for 30 min, and the peptide resin was washed extensively with 2-propanol and  $\text{CH}_2\text{Cl}_2$  and dried overnight in vacuo over  $\text{P}_2\text{O}_5$ .

Each of the labeled melanostatins was cleaved from the resin by treatment with 10 mL of 9:1 HF:anisole with stirring at 0 °C for 1 h. The HF was evaporated and the resin was extracted with 5 mL of diethyl ether and filtered on a fritted funnel. The resin was washed four times each with 5 mL of ether. The filtered resin was then washed five times each with 5 mL of 50% acetic acid. The acetic acid washings were combined, diluted with water, frozen, and lyophilized. The dried peptide residue was dissolved in water, frozen, and lyophilized again to remove residual anisole. Except for crystallization (vide infra), the labeled melanostatins were used without purification. The labeled melanostatins were characterized by TLC, FAB mass spectrometry, 300-MHz  $^1\text{H}$  NMR, and, for the  $^{13}\text{C}$ -labeled peptides, by 75-MHz  $^{13}\text{C}$  NMR. All of the analytical data were consistent with the expected products and with previously published characterizations.<sup>15</sup>

**Preparation of Crystalline Samples of Melanostatin for REDOR.** Solid solutions of labeled melanostatin in natural-abundance melanostatin were prepared by dissolving the labeled melanostatin in a minimal volume of MeOH and transferring the resulting solution to a vial containing an excess of solid, unlabeled tripeptide. After complete dissolution by gentle heating, the solution was allowed to cool. Crystallization occurred at room temperature as the MeOH evaporated. In some experiments, the inclusion of a small amount of water was found to slow the evaporation of solvent, leading to larger crystals. The crystals were then dried in vacuo over  $\text{P}_2\text{O}_5$ .

**REDOR NMR.** Rotational-echo double-resonance (REDOR)<sup>4,5</sup> is a solid-state NMR technique that permits the accurate measurement of through-space carbon-to-nitrogen distances between selectively  $^{13}\text{C}$ - and  $^{15}\text{N}$ -enriched sites. REDOR distances,  $r_{\text{CN}}$ , are calculated from measured heteronuclear dipolar constants,  $D_{\text{CN}}$ , according to the following equation:<sup>16</sup>

$$r_{\text{CN}} = \left( \frac{\gamma_C \gamma_N \hbar}{D_{\text{CN}} 2\pi} \right)^{1/3}$$

where  $\gamma_C$  and  $\gamma_N$  are the gyromagnetic ratios of  $^{13}\text{C}$  and  $^{15}\text{N}$ , respectively. In normal cross-polarization magic-angle spinning experiments,<sup>17</sup>  $^{13}\text{C}$ - $^{15}\text{N}$

dipolar couplings are removed by magic-angle spinning and do not effect the spectrum of the observed nucleus. In REDOR,  $\pi$  pulses applied synchronously with the rotation of the rotor serve to reintroduce the effect of these dipolar couplings.

The pulse sequence used to collect the REDOR  $^{13}\text{C}$  NMR data is shown in Figure 1. This sequence differs from the original REDOR pulse sequence<sup>4</sup> in that  $\pi$  pulses alternate between  $^{13}\text{C}$  and  $^{15}\text{N}$  rf channels. On alternate scans of the experiment, the  $\pi$  pulses on the nitrogen channel are either applied or omitted. Signals from alternate scans are accumulated and Fourier-transformed separately. When applied, the  $^{15}\text{N}$   $\pi$  pulses cause a partial dephasing of  $^{13}\text{C}$  signal due to the  $^{13}\text{C}$ - $^{15}\text{N}$  dipolar coupling, leading to a loss in  $^{13}\text{C}$  signal intensity. The magnitude of this signal loss,  $\Delta S$ , is determined by differencing spectra from the experiments with and without  $^{15}\text{N}$   $\pi$  pulses. The ratio of this difference to the signal from the isotopically enriched site alone ( $S_0$ ),  $\Delta S/S_0$ , depends on  $D_{\text{CN}}$  and two experimental parameters: (i) the spinning rate,  $\nu_R$  and (ii) the number of rotor periods of  $^{13}\text{C}$ - $^{15}\text{N}$  dipolar coupling evolution,  $N_C$ .<sup>5</sup> The analytical relationship between  $\Delta S/S_0$  and the parameters  $D_{\text{CN}}$ ,  $\nu_R$ , and  $N_C$  can be written in closed form.<sup>5</sup> However, in powder samples the expression relating these parameters must be integrated over all possible molecular orientations, and a computer is required for its evaluation.

**Experimental NMR.** REDOR  $^{13}\text{C}$  NMR experiments were performed on a home-built spectrometer operating at a  $^1\text{H}$  Larmor frequency of 127.0 MHz. Samples were spun at the magic angle (54.7°) with respect to the static magnetic field in a double-bearing rotor system<sup>19</sup> at a rate of 3 kHz. The REDOR spectra shown in Figures 2 and 3 were acquired over time periods of up to 3 days each. Electronic feedback circuits on the spectrometer permit us to control  $\nu_R$  to within  $\pm 3$  Hz and the field strengths,  $H_1$ , on each of the three rf channels to within  $\pm 0.25\%$ . This control circuitry helps to provide excellent long-term spectrometer stability, allowing us to produce reliable difference spectra that are necessary for accurate distance measurements. Carbon NMR spectra were obtained at 31.94 MHz following 2-ms matched, 50-kHz  $^1\text{H}$ - $^{13}\text{C}$  cross-polarization contacts. Proton decoupling fields were 110 kHz during the dipolar evolution period and 80 kHz during data acquisition. The amplitude of the  $^{15}\text{N}$  rf field was 35 kHz. Phases of both the  $^{13}\text{C}$  and  $^{15}\text{N}$   $\pi$  pulses were cycled according to the XY-8 (xyxyxyx) scheme<sup>20</sup> to minimize off-resonance effects.<sup>18,21</sup>  $\Delta S/S_0$  values were computed as the ratios of peak heights in the REDOR spectra.

**Conformational Analysis.** Three of the REDOR-determined  $r_{\text{CN}}$ 's depend upon backbone dihedral angles in melanostatin: [ $^{15}\text{N}$ ]Leu to [ $^{13}\text{C}$ ]Gly, ( $\psi_{\text{Leu}}$ ); [ $^{13}\text{C}$ ]Pro to [ $^{15}\text{N}$ ]Gly, ( $\phi_{\text{Leu}}$ ,  $\psi_{\text{Leu}}$ ); [ $^{15}\text{N}$ ]Leu to [ $^{13}\text{C}$ ]Gly, ( $\phi_{\text{Gly}}$ ,  $\psi_{\text{Leu}}$ ). Carbon-to-nitrogen distances were calculated as a function of these dihedral angles using Insight II (v 2.1.0, Biosym, San Diego, CA). Regions of dihedral space that satisfied single  $r_{\text{CN}}$  distance constraints were identified using FORTRAN programs written for that purpose. Variations of these programs determined those regions of ( $\phi_{\text{Leu}}$ ,  $\psi_{\text{Leu}}$ ) and ( $\phi_{\text{Gly}}$ ,  $\psi_{\text{Leu}}$ ) space that simultaneously satisfy both the appropriate single  $r_{\text{CN}}$  distance constraint and the constraint on  $\psi_{\text{Leu}}$  imposed by the [ $^{15}\text{N}$ ]Leu to [ $^{13}\text{C}$ ]Gly distance. Similarly, ( $\phi_{\text{Gly}}$ ,  $\psi_{\text{Leu}}$ ) pairs that simultaneously satisfy three constraints were found by taking the intersection of the region of ( $\phi_{\text{Gly}}$ ,  $\psi_{\text{Leu}}$ ) space allowed by the [ $^{15}\text{N}$ ]Leu to [ $^{13}\text{C}$ ]Gly distance with the range of allowed  $\psi_{\text{Leu}}$  values determined from the two constraints on ( $\phi_{\text{Leu}}$ ,  $\psi_{\text{Leu}}$ ). For comparison with the X-ray structure, we used coordinates determined on a crystalline sample that had been used for REDOR measurements.<sup>12</sup> The dihedral angles  $\phi_{\text{Leu}}$ ,  $\psi_{\text{Leu}}$ , and  $\phi_{\text{Gly}}$  in this structure differ by less than 2° from the values published by Reed and Johnson.<sup>11</sup>

## Results

REDOR  $^{13}\text{C}$  NMR spectra of Pro-[ $^{13}\text{C}$ ,  $^{15}\text{N}$ ]Leu-Gly-NH<sub>2</sub> and [ $^{13}\text{C}$ ]Pro-Leu-[ $^{15}\text{N}$ ]Gly-NH<sub>2</sub> are shown in Figure 2. Each of these labeled melanostatins was diluted in natural-abundance tripeptide ([ $^{13}\text{C}$ ,  $^{15}\text{N}$ ]Leu sample, 1:7; [ $^{13}\text{C}$ ]Pro/[ $^{15}\text{N}$ ]Gly sample, 1:9). Figure 2 (left) shows the REDOR results for the fixed distance [ $^{13}\text{C}$ ,  $^{15}\text{N}$ ]Leu sample collected with 16 rotor cycles

(17) (a) Schaefer, J.; Stejskal, E. O. *J. Am. Chem. Soc.* **1976**, *98*, 1031. (b) Fyfe, C. A. *Solid-State NMR for Chemists*; CFC Press: Guelph, 1983. (c) Mehring, M. *High-Resolution NMR in Solids*; Springer-Verlag: New York, 1983.

(18) Gullion, T.; Schaefer, J.; Baker, D. B.; Lizak, M.; Conradi, M. S. Presented at the 31st Experimental NMR Conference, Asilomar, CA, April, 1990.

(19) Schaefer, J.; Garbow, J. R.; Stejskal, E. O.; Lefalar, J. *Macromolecules* **1987**, *20*, 1271.

(20) Gullion, T.; Baker, D. B.; Conradi, M. S. *J. Magn. Reson.* **1990**, *89*, 479.

(21) Gullion, T.; Schaefer, J. *J. Magn. Reson.* **1991**, *92*, 439.

(15) (a) Hruby, V. J.; Brewster, A. I.; Glasel, J. A. *Proc. Natl. Acad. Sci. U.S.A.* **1971**, *68*, 450. (b) Deslauriers, R.; Walter, R.; Smith, I. C. P. *FEBS Lett.* **1973**, *37*, 27. (c) Higashijima, T.; Tasumi, M.; Miyazawa, T. *FEBS Lett.* **1975**, *57*, 175. (d) Higashijima, T.; Tasumi, M.; Miyazawa, T.; Miyoshi, M. *Eur. J. Biochem.* **1978**, *89*, 543.

(16) Abragam, A. *Principles of Nuclear Magnetism*; Oxford University Press: London, 1961.

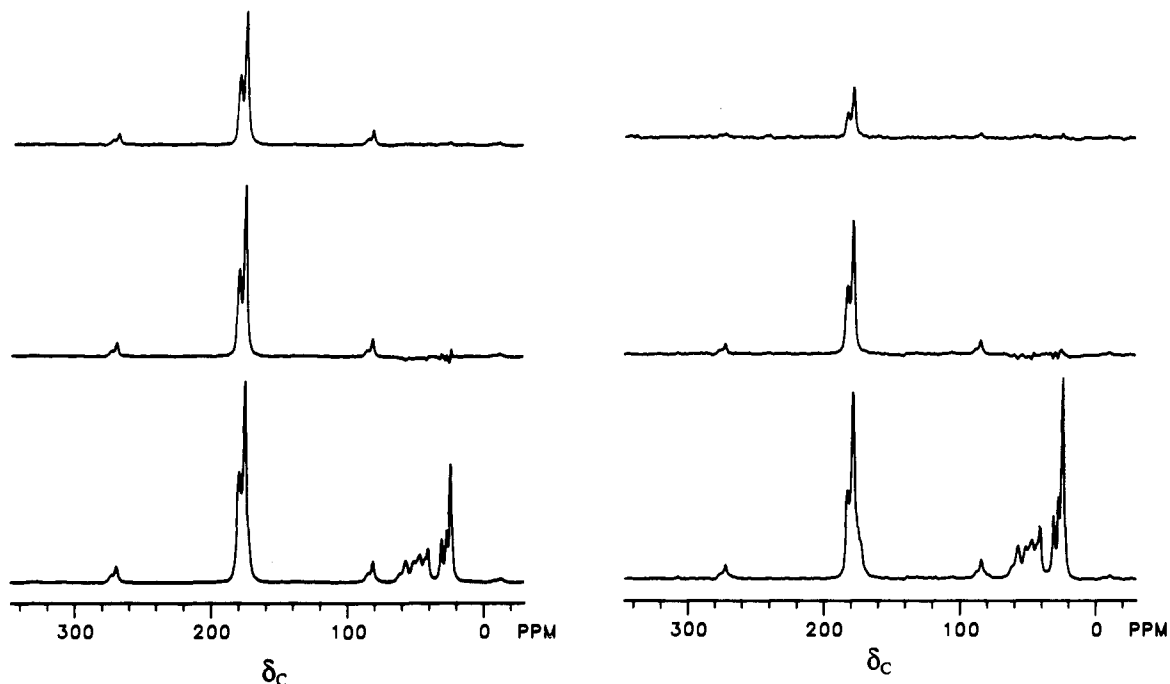


**Figure 2.** REDOR  $^{13}\text{C}$  NMR spectra of (left) Pro-[ $1\text{-}^{13}\text{C},^{15}\text{N}$ ]Leu-Gly-NH $_2$  in natural-abundance tripeptide (1:7; 179 mg total sample weight; 20 000 accumulated scans) and (right) [ $1\text{-}^{13}\text{C}$ ]Pro-Leu-[ $^{15}\text{N}$ ]Gly-NH $_2$  in natural-abundance tripeptide (1:9; 110 mg total sample weight, 60 000 accumulated scans): (bottom) echo spectra of full sample; (middle) echo spectra following subtraction of signals due to natural-abundance Pro-Leu-Gly-NH $_2$ ; (top) REDOR difference. Spectra were collected using the pulse sequence of Figure 1 with  $\nu_R = 3$  kHz: (left)  $N_C = 16$ , (right)  $N_C = 32$ .

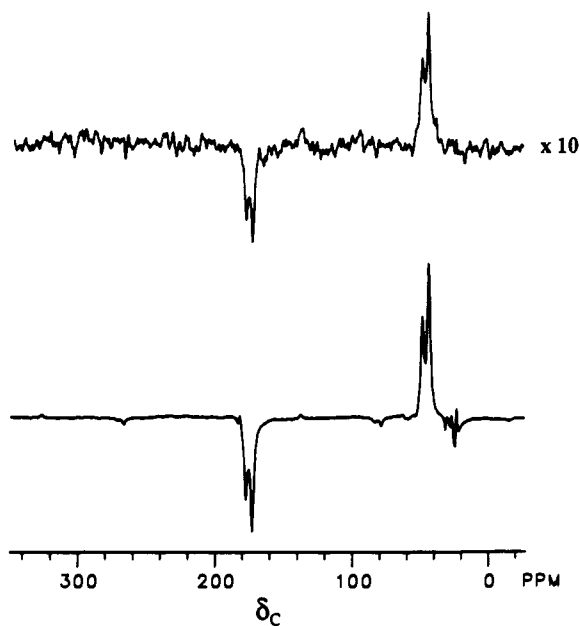


**Figure 3.** REDOR  $^{13}\text{C}$  NMR spectra of Pro-[ $^{15}\text{N}$ ]Leu-[ $1\text{-}^{13}\text{C}$ ]Gly-NH $_2$  in natural-abundance tripeptide (1:49; 512 mg total sample weight; 200 000 accumulated scans) and Pro-[ $^{15}\text{N}$ ]Leu-[ $2\text{-}^{13}\text{C}$ ]Gly-NH $_2$  in natural-abundance tripeptide (1:49; 541 mg total sample weight; 130 000 accumulated scans): (bottom) difference of echo spectra of full samples showing signals from labeled carbons only; (top) difference of REDOR difference signals. Spectra for each sample were collected using the pulse sequence of Figure 1 with  $\nu_R = 3$  kHz,  $N_C = 32$ .

of dipolar dephasing ( $N_C = 16$ ). The bottom spectra is that of the full sample collected in the absence of all  $^{15}\text{N}$   $\pi$  pulses and shows signals arising from the  $^{13}\text{C}$ -enriched and natural-abundance carbonyl carbons ( $\delta_c$  172–178 ppm), and natural-abundance methyl ( $\delta_c$  23 ppm), methylene ( $\delta_c$  27, 31 ppm), other side-chain aliphatic ( $\delta_c$  40–50 ppm), and  $\text{C}_\alpha$  ( $\delta_c$  50–60 ppm) carbons in the tripeptide. Signals near 80 ppm and 270 ppm are spinning sidebands, which result from the mechanical sample rotation and occur at  $\pm$  the 3-kHz spinning speed. Figure 2 (left, middle) shows

the  $^{13}\text{C}$  signal due to the labeled leucyl carbonyl carbon only. This spectrum was obtained by subtracting the spectrum of a natural-abundance melanostatin sample (data not shown) collected under identical experimental conditions. The spectrum of this labeled carbon is an asymmetric doublet, with the splitting due to dipolar coupling between the carbonyl carbon and directly bonded  $^{14}\text{N}$  spin in the peptide bond. Because of the quadrupolar nature of  $^{14}\text{N}$ , this dipolar coupling is not completely removed by magic-angle spinning.<sup>22</sup> The REDOR difference signal,  $\Delta S$ , is shown in Figure 2 (left, top). The value of  $\Delta S/S_0$  measured from these spectra is 0.791.

In addition to the effects of dipolar couplings between the labeled  $^{13}\text{C}$  and  $^{15}\text{N}$  sites, REDOR  $\Delta S/S_0$  values also receive contributions from natural-abundance  $^{13}\text{C}$  spins (1.1%) that are near the enriched nitrogens and natural-abundance  $^{15}\text{N}$  spins (0.33%) that are near the enriched carbons. Although these spins represent only a small fraction of the total nuclei, their proximity to the labeled sites results in strong carbon–nitrogen dipolar coupling, producing observable contributions to the REDOR difference signals. The relative importance of these natural-abundance REDOR differences increases as the distance between the labeled sites increases. Long distances produce only small REDOR difference signals, and  $\Delta S$  due to natural-abundance spins can be comparable in magnitude to that from the labeled  $^{13}\text{C},^{15}\text{N}$  pair. Since the natural-abundance contributions are due to known, fixed distances, their effects can be calculated exactly and the measured  $\Delta S/S_0$  ratios adjusted accordingly. Calculations of natural-abundance corrections to the REDOR signals for each of the labeled melanostatins are described in the Appendix.

For Pro-[ $1\text{-}^{13}\text{C},^{15}\text{N}$ ]Leu-Gly-NH $_2$ , natural-abundance contributions to  $\Delta S/S_0$  total 0.014, and the corrected  $\Delta S/S_0$  value for this sample is 0.777. From this  $\Delta S/S_0$  value, the spinning speed (3 kHz) and the number of cycles of dipolar evolution ( $N_C = 16$ ), we calculate a  $D_{\text{CN}}$  of 199 Hz.

Figure 2 (right) shows the corresponding REDOR  $^{13}\text{C}$  NMR spectra for [ $1\text{-}^{13}\text{C}$ ]Pro-Leu-[ $^{15}\text{N}$ ]Gly-NH $_2$ , collected with  $N_C = 32$ . The internuclear distance between the labeled sites in this

(22) (a) Olivieri, A. C.; Frydman, L.; Diaz, L. E. *J. Magn. Reson.* **1987**, *75*, 50. (b) Hexem, J. G.; Frey, M. H.; Opella, S. J. *J. Am. Chem. Soc.* **1981**, *103*, 224.

Table I. REDOR  $^{13}\text{C}$  NMR of  $^{13}\text{C}$ ,  $^{15}\text{N}$ -Enriched Melanostatins

$^{13}\text{C}$ site	$^{15}\text{N}$ site	$N_{\text{C}}$	$\Delta S/S_0^{a,b}$	$D_{\text{CN}}$ (Hz)	$r_{\text{CN}}, \text{\AA}$		
					REDOR	X-ray <sup>12</sup>	$(\phi = \psi = 180^\circ)^{26}$
[1- $^{13}\text{C}$ ]Leu	[ $^{15}\text{N}$ ]Leu	16	0.777	199	2.43	2.42	2.45
[1- $^{13}\text{C}$ ]Pro	[ $\alpha$ - $^{15}\text{N}$ ]Gly	32	0.346	57	3.69	3.70	5.09
[2- $^{13}\text{C}$ ]Gly	[ $^{15}\text{N}$ ]Leu	32	0.081	26	4.78	4.68	5.02
[1- $^{13}\text{C}$ ]Gly	[ $^{15}\text{N}$ ]Leu	32	0.073	25	4.87	4.97	6.24

<sup>a</sup> Computed as the ratio of measured peak heights. <sup>b</sup> Includes correction for natural-abundance terms, as described in the Appendix.

molecule depends upon the dihedral angles  $\phi_{\text{Leu}}$  and  $\psi_{\text{Leu}}$ . The presentation of data in this figure is the same as in Figure 2 (left), and the  $\Delta S/S_0$  ratio is measured to be 0.374. Natural-abundance corrections (Appendix) reduce the value of  $\Delta S/S_0$  to 0.346, corresponding to a carbon-nitrogen dipolar coupling of 57 Hz.

Figure 3 shows REDOR  $^{13}\text{C}$  NMR spectra of two different [ $^{15}\text{N}$ ]Leu-labeled melanostatins: Pro-[ $^{15}\text{N}$ ]Leu-[1- $^{13}\text{C}$ ]Gly-NH<sub>2</sub> and Pro-[ $^{15}\text{N}$ ]Leu-[2- $^{13}\text{C}$ ]Gly-NH<sub>2</sub>. Each of these samples was diluted 1:49 in natural-abundance tripeptide. The reason for this additional dilution compared with the first pair of melanostatin samples is discussed below. The data in Figure 3 are presented in a somewhat different format than in Figure 2. Because the [1- $^{13}\text{C}$ ]Gly-enriched melanostatin sample is natural-abundance in the C <sub>$\alpha$</sub>  position of Gly and vice-versa for the [2- $^{13}\text{C}$ ]Gly-enriched sample, these two samples can serve to experimentally correct each other's natural-abundance  $^{13}\text{C}$  contributions to both the full-echo signal and  $\Delta S/S_0$ . This experimental self-correction for natural-abundance REDOR difference signals is necessary, because there are contributions to  $\Delta S$  from natural-abundance, side-chain leucyl carbons that are not chemical-shift resolved from the labeled [2- $^{13}\text{C}$ ]Gly carbon. The partial overlap of carbon signals makes these contributions to  $\Delta S/S_0$  difficult to calculate. Instead they are experimentally removed by a double-difference technique.

Figure 3 (bottom) shows the difference spectrum formed by subtracting the full spectrum of the [1- $^{13}\text{C}$ ]Gly/[ $^{15}\text{N}$ ]Leu sample from that of the [2- $^{13}\text{C}$ ]Gly/[ $^{15}\text{N}$ ]Leu sample. Signal from the enriched [2- $^{13}\text{C}$ ]Gly appears as a positive-going doublet in this spectrum; signal from the enriched [1- $^{13}\text{C}$ ]Gly position as a negative-going signal. Figure 3 (top) shows the difference spectrum of the REDOR difference spectra for these two samples. The  $\Delta S/S_0$  ratios from these difference spectra are measured to be 0.080 (carbonyl) and 0.088 (C <sub>$\alpha$</sub> ). Despite the double-difference method that produced these spectra, these  $\Delta S/S_0$  values still include contributions from natural-abundance  $^{15}\text{N}$ 's that are near the labeled carbons (Appendix). Correcting the measured values, we calculate carbon-nitrogen dipolar couplings of 25 Hz and 26 Hz for the carbonyl and C <sub>$\alpha$</sub> , respectively.

The double-difference method illustrated in Figure 3 will be generally useful anytime that contributions to REDOR difference signals arising from natural-abundance carbons cannot be easily calculated. Examples include the present case, in which these natural-abundance signals are only partially chemical-shift resolved, and cases where natural-abundance contributions are unknown, as may occur for a bound, labeled inhibitor that is near naturally-occurring  $^{13}\text{C}$  spins in the active site of an enzyme.

The results of the REDOR experiments are summarized in Table I and include  $\Delta S/S_0$  and  $D_{\text{CN}}$ 's between labeled sites for each of the four melanostatins. The carbon-nitrogen dipolar coupling measured for the Pro-[1- $^{13}\text{C}$ , $^{15}\text{N}$ ]Leu-Gly-NH<sub>2</sub> sample is approximately 10% smaller than the calculated rigid lattice value for this carbon-nitrogen distance of 2.42  $\text{\AA}$ .<sup>12</sup> Similar reductions in couplings have been observed in measurements of carbon-nitrogen<sup>6,23</sup> and carbon-proton<sup>24</sup> dipolar interactions and are attributed primarily to the effects of high-frequency librational and vibrational motions.<sup>25</sup> In an independent REDOR experiment,

we measured  $\Delta S/S_0$  for C <sub>$\alpha$</sub>  in a sample of [2- $^{13}\text{C}$ , $^{15}\text{N}$ ]Gly to be 0.42 ( $N_{\text{C}} = 8$ ). This REDOR difference translates into a  $D_{\text{CN}}$  of 875 Hz. In calculating internuclear distances from dipolar couplings in melanostatin, we have used this experimentally measured  $D_{\text{CN}}$  for the 1.48- $\text{\AA}$  C <sub>$\alpha$</sub> -N distance in glycine. Following this approach, we find excellent agreement in the [1- $^{13}\text{C}$ , $^{15}\text{N}$ ]Leu sample between the distance measured by REDOR and the distance known from the leucyl geometry (2.43  $\text{\AA}$  versus 2.42  $\text{\AA}$ ), thus validating the assumption that the averaging of dipolar couplings by high-frequency motions in melanostatin is similar to that in crystalline glycine. REDOR determined carbon-nitrogen distances are listed in Table I, along with the distances measured in our X-ray study of melanostatin<sup>12</sup> and those calculated for a fully extended conformation ( $\phi = \psi = 180^\circ$ ).<sup>26</sup>

Having taken into account both the natural-abundance contributions to these REDOR data and the effects of high-frequency molecular motions, the major uncertainty in the REDOR distances of Table I arises from errors in the experimentally measured values of  $\Delta S/S_0$ . For these melanostatin data, the signal-to-noise ratios are lowest, and the corresponding errors in  $\Delta S/S_0$  are highest, for the double-difference REDOR spectra of Figure 3. We estimate the uncertainties in  $\Delta S/S_0$  in these spectra to be  $\pm 0.005$ , corresponding to uncertainties of  $\sim 0.05$   $\text{\AA}$  in the determinations of the [ $^{15}\text{N}$ ]Leu-[2- $^{13}\text{C}$ ]Gly and [ $^{15}\text{N}$ ]Leu-[1- $^{13}\text{C}$ ]Gly distances. Experimental errors in the distance measurements for the fixed-distance and [1- $^{13}\text{C}$ ]Pro-[ $^{15}\text{N}$ ]Gly samples are smaller.

As noted above, the Pro-[ $^{15}\text{N}$ ]Leu-[1- $^{13}\text{C}$ ]Gly-NH<sub>2</sub> and Pro-[ $^{15}\text{N}$ ]Leu-[2- $^{13}\text{C}$ ]Gly-NH<sub>2</sub> samples whose spectra are shown in Figure 3 were each diluted 1:49 in natural-abundance tripeptide. Originally, these samples were prepared at a 1 part in 9 dilution, just like the [1- $^{13}\text{C}$ ]Pro labeled sample. Using these samples, we consistently measured a carbon-to-nitrogen distance in Pro-[ $^{15}\text{N}$ ]Leu-[1- $^{13}\text{C}$ ]Gly-NH<sub>2</sub> that was  $\sim 0.15$   $\text{\AA}$  shorter than that reported in Table I and nearly 0.3  $\text{\AA}$  shorter than that reported by X-ray.<sup>11</sup> To clarify this situation, X-ray crystallography was performed on a single-crystal grown from the Pro-[ $^{15}\text{N}$ ]Leu-[2- $^{13}\text{C}$ ]Gly-NH<sub>2</sub> sample. This study revealed that, in melanostatin, there is an intermolecular leucine nitrogen to glycine carbonyl-carbon distance of 3.63  $\text{\AA}$ .<sup>12</sup> Even at 1:9 dilution, the intermolecular contribution to  $\Delta S/S_0$  from labeled melanostatin neighbors is enough to cause a sizable error in the measured intramolecular distance. We estimate that, at the 1:49 dilution, intermolecular effects cause an error of less than 0.05  $\text{\AA}$  in our determination of the carbon-nitrogen distance. Although intermolecular effects are always a potential source of error, experimental strategies such as the dilution study reported here make it possible to detect and eliminate these effects. Moreover, we expect intermolecular effects to be less important in determining the conformations of most bound ligands, where the macromolecule itself serves to isolate the labeled ligand molecules.

## Discussion

The carbon-to-nitrogen distances calculated from the REDOR data (Table I) span a range from 2.4  $\text{\AA}$  to 4.9  $\text{\AA}$  and include distances involving both carbonyl and aliphatic carbons. The REDOR results compare favorably with the values derived from the X-ray structure and indicate that carbon-to-nitrogen distances can be accurately measured using the technique. Perhaps as importantly, the distances determined in this study provide con-

(23) Bork, V.; Gullion, T.; Hing, A.; Schaefer, J. *J. Magn. Reson.* **1990**, *88*, 523.

(24) (a) Munowitz, M. G.; Griffin, R. G. *J. Chem. Phys.* **1982**, *76*, 2848. (b) Schaefer, J.; McKay, R. A.; Stejskal, E. O.; Dixon, W. T. *J. Magn. Reson.* **1983**, *52*, 123.

(25) (a) Torchia, D.; Szabo, A. *J. Magn. Reson.* **1982**, *49*, 107. (b) Henry, E. R.; Szabo, A. *J. Chem. Phys.* **1985**, *82*, 4753.

(26) Calculated assuming rigid-residue geometry provided with Insight II, Version 2.1.0, Biosym Technologies of San Diego.

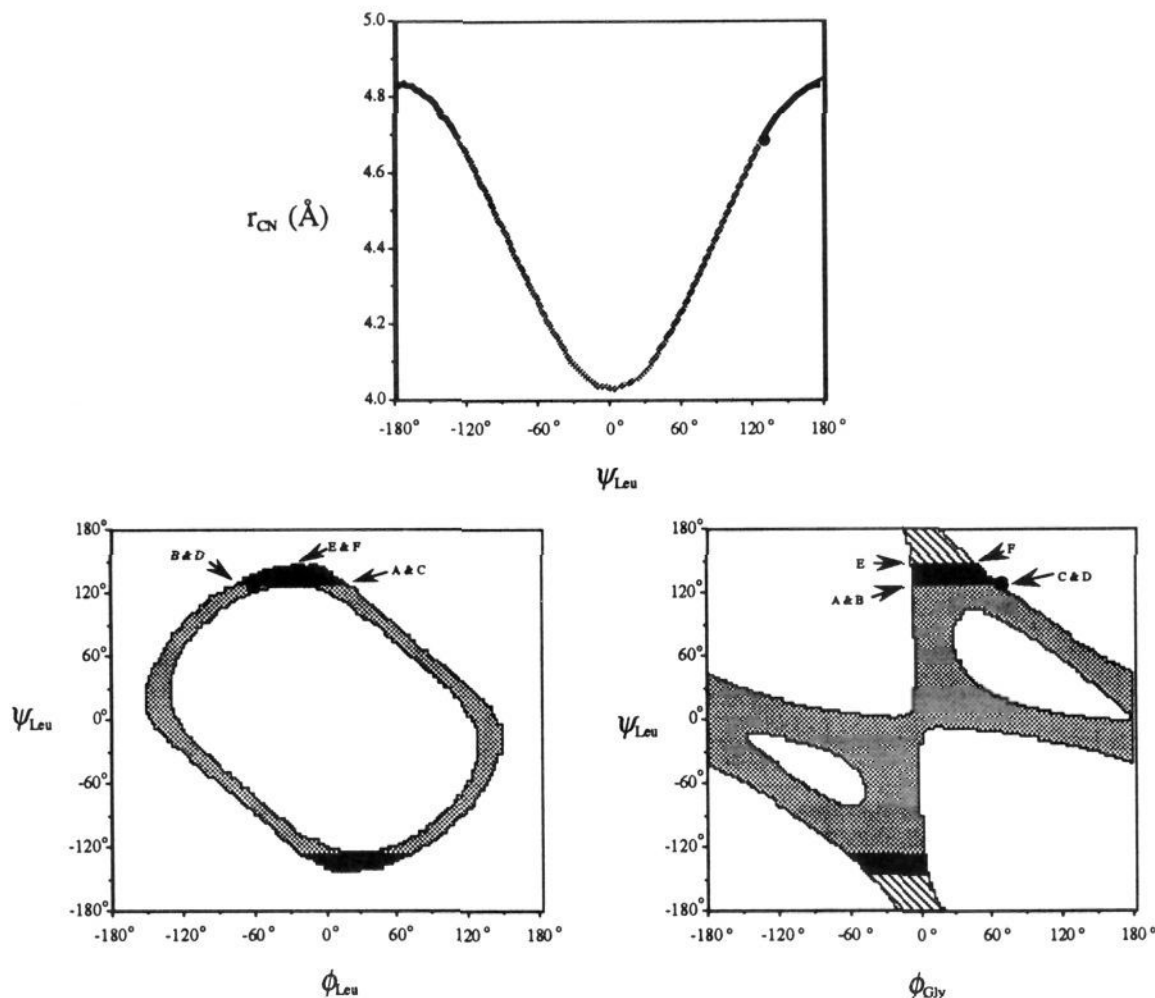


**Figure 4.** Conformational maps, showing how the distances measured in REDOR experiments constrain the allowed values of  $\phi_{Leu}$ ,  $\psi_{Leu}$ , and  $\phi_{Gly}$  in melanostatin. In each map, the X-ray conformation<sup>12</sup> is indicated by a bull's-eye. (Top) [<sup>15</sup>N]Leu to [<sup>13</sup>C]Gly distance as a function of  $\psi_{Leu}$ , using 2.5° increments (144 conformations). Black lines show those angles (42 conformations) that are consistent with the measured REDOR distance (4.78 ± 0.1 Å); the gray line indicates angles (102 conformations) that are excluded by the REDOR measurement. (Bottom, left) Constraints on the dihedral angles  $\phi_{Leu}$  and  $\psi_{Leu}$  imposed by the REDOR-measured [<sup>13</sup>C]Pro to [<sup>15</sup>N]Gly distance were determined by examining this distance for 20736 discrete conformations (2.5° increments for each angle). The gray and black (nonwhite) annulus shows those conformations (1870) that are consistent with the measured [<sup>13</sup>C]Pro to [<sup>15</sup>N]Gly distance (3.69 ± 0.1 Å); white areas are angles (18866) that are excluded by the REDOR measurement. The two black patches indicate values of  $\phi_{Leu}$  and  $\psi_{Leu}$  (328 conformations) that are consistent with both REDOR distance constraints. The notations A–F refer to specific conformations that span the allowed regions (upper black patches; see also Figure 5 (top) and text). (Bottom, right) Constraints on the dihedral angles  $\psi_{Leu}$  and  $\phi_{Gly}$  (20736 conformations, 2.5° increments) imposed by all three of the conformationally-dependent REDOR distances. Nonwhite areas are conformations (5738) that are consistent with the measured [<sup>15</sup>N]Leu to [<sup>13</sup>C]Gly distance. The [<sup>15</sup>N]Leu to [<sup>13</sup>C]Gly distance (4.78 ± 0.1 Å) further limits the allowed conformation to the black and cross-hatched areas (339 + 462 = 801 conformations). The black areas are the conformations (339) allowed by the two Leu-to-Gly distance constraints that also have values for  $\psi_{Leu}$  that are permitted in Figure 4 (bottom, left). The labels A–F are as described above.

straints on the values of the rotatable, backbone dihedral angles  $\phi_{Leu}$ ,  $\psi_{Leu}$ , and  $\phi_{Gly}$ . Here we discuss how these constraints combine with simple energetic considerations to define the backbone conformation of melanostatin.

Assuming rigid-residue geometry and a trans peptide bond, the distance between the carbon and nitrogen labels in Pro-[<sup>15</sup>N]-Leu-[<sup>13</sup>C]Gly-NH<sub>2</sub> only depends upon the angle  $\psi_{Leu}$ . Figure 4 (top) shows a plot of this distance as a function of  $\psi_{Leu}$ . The black portions of the curve are those values of  $\psi_{Leu}$  that satisfy the REDOR distance (4.78 Å) to within ±0.1 Å;<sup>27</sup> the gray curve shows values that are excluded by the REDOR data. This one distance constrains the allowed values of  $\psi_{Leu}$  to two symmetrically placed regions that together represent 29% of  $\psi_{Leu}$ 's total dihedral space. Similarly, the distance between the carbon and nitrogen labels in [<sup>13</sup>C]Pro-Leu-[<sup>15</sup>N]Gly-NH<sub>2</sub> varies with rotation about

$\phi_{Leu}$  and  $\psi_{Leu}$ . The conformational constraints on  $\phi_{Leu}$  and  $\psi_{Leu}$  imposed by this  $r_{CN}$  are illustrated in Figure 4 (bottom, left), with the allowed regions shown in black and gray (nonwhite) and the excluded regions shown in white. The experimental distance (3.69 ± 0.1 Å) limits the possible conformations to an annular region which is 9% of the total ( $\phi_{Leu}$ ,  $\psi_{Leu}$ ) dihedral space. The result of combining the conformational constraints imposed by the REDOR experiments on Pro-[<sup>15</sup>N]Leu-[<sup>13</sup>C]Gly-NH<sub>2</sub> and [<sup>13</sup>C]Pro-Leu-[<sup>15</sup>N]Gly-NH<sub>2</sub> is shown in black in this figure. These constraints can be conveniently thought of as the intersection of the  $\psi_{Leu}$  regions allowed by the single  $r_{CN}$  constraints (i.e., the intersection of the black regions of Figure 4 (top) and the nonwhite region of Figure 4 (bottom, left)). The two black patches, describing those dihedral angle values that simultaneously satisfy both distance constraints, represent only 2% of the total ( $\phi_{Leu}$ ,  $\psi_{Leu}$ ) dihedral space.

A similar analysis of ( $\phi_{Gly}$ ,  $\psi_{Leu}$ ) conformational space, shown in Figure 4 (bottom, right), indicates that (i) the [<sup>15</sup>N]Leu to [<sup>13</sup>C]Gly  $r_{CN}$  limits the allowed conformations to the nonwhite

(27) The uncertainty in all of the REDOR distances was previously estimated to be ≤0.05 Å. For the conformational analysis, we have assumed an uncertainty of ±0.1 Å throughout, thus providing a safe margin of error.

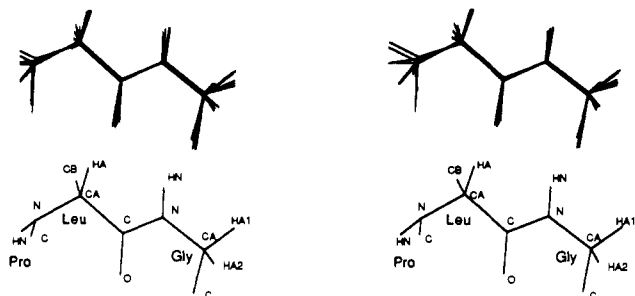


**Figure 5.** Stereo drawing of that portion of the melanostatin structure which depends on the dihedral angles  $\phi_{\text{Leu}}$ ,  $\psi_{\text{Leu}}$ , and  $\phi_{\text{Gly}}$ . (Top) Six conformations (A through F) were chosen to represent the extremes of the allowed regions (upper black patches) of Figure 4 (middle and bottom). These effectively represent the breadth of the conformational family defined by (i) the REDOR constraints on  $\phi_{\text{Leu}}$ ,  $\psi_{\text{Leu}}$ , and  $\phi_{\text{Gly}}$  and (ii) conservative energetic considerations (see text). The conformers were superimposed in order to yield the minimum RMSD for the 14-atom fragments shown. The pair-wise average minimum RMSD  $\pm$  std dev was  $0.498 \pm 0.149$  Å. The dihedral angles for A through F, in the order  $\phi_{\text{Leu}}$ ,  $\psi_{\text{Leu}}$ , and  $\phi_{\text{Gly}}$  were (A)  $17.5^\circ$ ,  $130^\circ$ ,  $-5^\circ$ ; (B)  $-70^\circ$ ,  $130^\circ$ ,  $-5^\circ$ ; (C)  $17.5^\circ$ ,  $130^\circ$ ,  $65^\circ$ ; (D)  $-70^\circ$ ,  $130^\circ$ ,  $65^\circ$ ; (E)  $-25^\circ$ ,  $145^\circ$ ,  $-5^\circ$ ; (F)  $-25^\circ$ ,  $145^\circ$ ,  $47.5^\circ$ . (Bottom) The X-ray conformation<sup>12</sup> of the 14-atom fragment of melanostatin shown in the same orientation as the REDOR conformer family. The pair-wise average minimum RMSD  $\pm$  std dev between each of the REDOR structures A through F with the X-ray structure is  $0.437 \pm 0.224$  Å. The dihedral angles in the X-ray structure, in the order  $\phi_{\text{Leu}}$ ,  $\psi_{\text{Leu}}$ , and  $\phi_{\text{Gly}}$ , were  $-60^\circ$ ,  $128^\circ$ , and  $70^\circ$ .

areas (28% of the total); (ii) a second constraint, the [ $^{15}\text{N}$ ]Leu to [ $^{13}\text{C}$ ]Gly  $r_{\text{CN}}$ , excludes the gray region, leaving 4% of the total as allowed (black plus cross-hatched regions); and (iii) a third constraint, introduced by limiting the values of  $\psi_{\text{Leu}}$  to those permitted in Figure 4 (bottom, left), further narrows the allowed regions to the two black patches (ca. 2% of the total). In the analysis of  $(\phi_{\text{Gly}}, \psi_{\text{Leu}})$ , the first distance is used as an explicit limitation, while the remaining two distances function indirectly by limiting the allowed values of  $\psi_{\text{Leu}}$ . The black patches represent the intersection of the limited  $\psi_{\text{Leu}}$  values of Figure 4 (bottom, left) with those permitted by the [ $^{15}\text{N}$ ]Leu to [ $^{13}\text{C}$ ]Gly  $r_{\text{CN}}$ .

To this point in the conformational analysis, only three simple assumptions have been made: (i) melanostatin exists in a unique conformation, (ii) melanostatin can be adequately described by standard rigid-residue geometry with trans peptide bonds, and (iii) the REDOR distances are accurate to within  $\pm 0.1$  Å. The conformational analysis can be extended, however, by considering conformational energy maps for the nonglycine amino acids.<sup>28</sup> The lower black patch (i.e.,  $\phi_{\text{Leu}} \sim -20^\circ$  to  $+70^\circ$ ,  $\psi_{\text{Leu}} \sim -130^\circ$  to  $-140^\circ$ ) of Figure 4 (bottom, left) corresponds to a high-energy region of conformational space. Even if the possible effects of crystal packing are considered, this region is unlikely to be populated. Therefore, the lower black patches in Figure 4 (middle and bottom) can be excluded, leaving a small family of allowed conformers described by the upper black patches in these plots, (i.e.,  $\phi_{\text{Leu}}$  from  $-70^\circ$  to  $+20^\circ$ ,  $\psi_{\text{Leu}}$  from  $130^\circ$  to  $145^\circ$ , and  $\phi_{\text{Gly}}$  from  $-5^\circ$  to  $+65^\circ$ ). Since there will normally be little or no information on intermolecular contacts, the use of intramolecular energy as a criteria for further restricting REDOR-derived conformations should be limited to cases like this, where the energy is prohibitively high.

Of the three dihedral angles considered here,  $\psi_{\text{Leu}}$  is the most restricted. This is reasonable since all three of the conformationally dependent distances determined in this study restrict its value, whereas the other two dihedrals are restricted by only one distance each. Figure 5 (top) depicts a minimum RMSD superposition of six molecular structures representing the points labeled A-F on the conformational maps of Figure 4. These structures, which show the 14-atom portion of melanostatin that depends on the angles  $\phi_{\text{Leu}}$ ,  $\psi_{\text{Leu}}$ , and  $\phi_{\text{Gly}}$ , illustrate the breadth of conformations

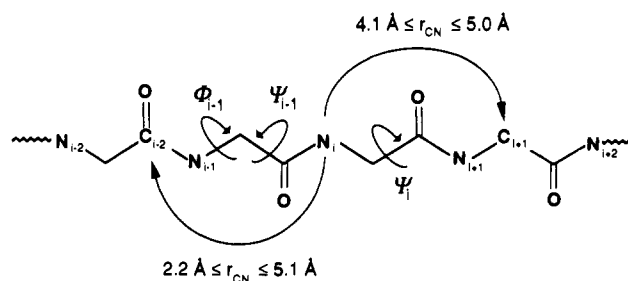


**Figure 6.** Isotopic labeling scheme for determining backbone dihedral angles using  $^{13}\text{C}$ ,  $^{15}\text{N}$ -REDOR NMR distance constraints. The region of interest in the peptide or protein is selected and an [ $\alpha$ - $^{15}\text{N}$ ]-labeled amino acid is placed at residue  $i$ . In the same molecule,  $^{13}\text{C}$  labels are placed in the carbonyl position of residue  $i-2$  and  $\text{C}_\alpha$  of residue  $i+1$ . The minimum and maximum distances between the labeled sites are within the range that can be measured with REDOR. REDOR experiments are thus guaranteed to provide two measurable carbon-nitrogen distances that constrain the  $\phi, \psi$  angles.

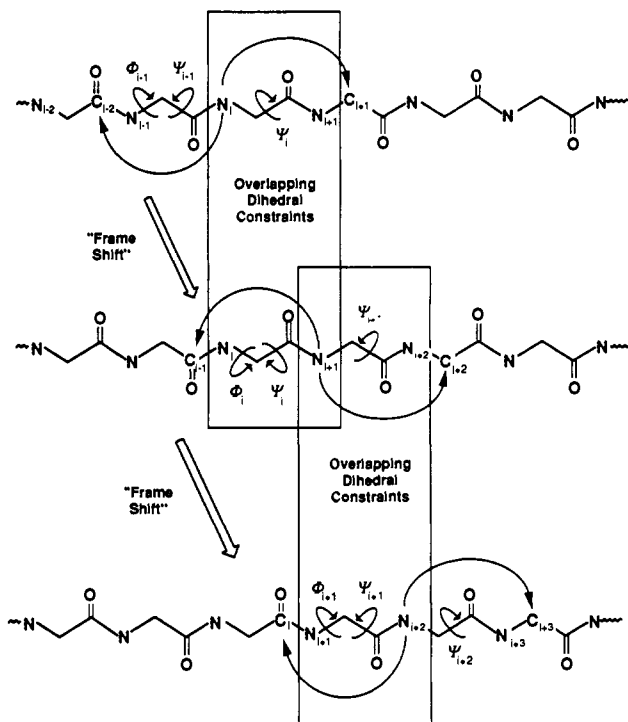


**Figure 7.** General strategy for mapping the backbone conformation of peptides or proteins using  $^{13}\text{C}$ ,  $^{15}\text{N}$ -REDOR NMR. As shown at the top of this figure, two  $^{13}\text{C}$  labels and a  $^{15}\text{N}$  are placed in the peptide backbone according to the scheme of Figure 5. REDOR experiments provide constraints on the angles  $\phi_{i-1}$  and  $\psi_{i-1}$ , and  $\psi_i$ . A frame-shift of the labeled triple along the backbone leads to overlapping dihedral angle constraints which can be used to map the conformation of the backbone.

defined by the upper black patches of Figure 4 (middle and bottom), i.e., the range of conformations that satisfy the REDOR data using geometrical information and very conservative energetic considerations. The pairwise, average minimum RMSD among the six structures is  $0.498 \pm 0.149$  Å (avg  $\pm$  std dev).

The X-ray conformation, shown in Figure 5 (bottom), is similar to that of a type II bend in which Leu and Gly occupy the central two positions. A 10-atom cycle is formed by a hydrogen bond (not shown) from the terminal-amide proton to the proline carbonyl. A comparison of the REDOR-derived and X-ray structures (Figure 5, top and bottom) clearly indicates a close correspondence for the backbone and pendant atoms running from Pro  $\text{N}_\alpha$  to Gly  $\text{C}_\alpha$ . The pairwise, average minimum RMSD between the REDOR fragment structures of Figure 5 (top) and the X-ray conformation is  $0.437 \pm 0.224$  Å (avg  $\pm$  std dev). Thus, REDOR data serve remarkably well to define the conformation of melanostatin. The remaining backbone dihedral angles,  $\psi_{\text{Pro}}$  and  $\psi_{\text{Gly}}$ , remain un-

(28) Zimmerman, S. S.; Pottle, M. S.; Nemethy, G.; Scheraga, H. A. *Macromolecules* 1977, 10, 1.

defined in the current study. Additional carbon-to-nitrogen constraints would be needed to establish these angles from NMR data.

The results of our work on melanostatin suggest a general strategy for using REDOR constraints to map the backbone conformations of peptides and proteins. This strategy, which is shown schematically in Figures 6 and 7, involves making carbon–nitrogen distance measurements for a series of triply-enriched peptides or proteins. The first step in the process is to choose a region of the peptide/protein to be mapped, and to place an [ $\alpha$ - $^{15}\text{N}$ ]-labeled amino acid at residue  $i$  (Figure 6). In the same molecule,  $^{13}\text{C}$  labels are placed in the carbonyl position of residue  $i - 2$  and the  $\alpha$ -carbon of residue  $i + 1$ . Since these two carbon sites are well separated from one another and their NMR signals are resolved, two  $r_{\text{CN}}$  can be measured simultaneously in this sample with a single REDOR experiment.

As indicated in Figure 6, the minimum and maximum distances between the labeled sites are within the range that can be measured by REDOR. Thus, REDOR experiments on this sample are guaranteed to provide two measurable, nontrivial carbon–nitrogen distances which will provide constraints on backbone dihedral angles. Each subsequent sample is then prepared by shifting the labeled  $^{13}\text{C}, ^{15}\text{N}, ^{13}\text{C}$  triple, residue by residue, up or down the protein chain, as illustrated in Figure 7. The distances measured in these *frame-shifted* samples provide a series of overlapping dihedral constraints, in a fashion analogous to the constraints imposed on  $\phi_{\text{Leu}}$  and  $\psi_{\text{Leu}}$  in melanostatin (Figure 4, middle), that will allow the complete backbone conformation to be mapped.

### Conclusions

In this paper, we have described the determination of the backbone conformation of the tripeptide melanostatin using distance constraints derived from  $^{13}\text{C}, ^{15}\text{N}$ -REDOR NMR experiments. Together with conservative energy considerations, the three conformationally dependent carbon–nitrogen distances measured using REDOR greatly restrict the allowed values for the dihedral angles  $\phi_{\text{Leu}}$ ,  $\psi_{\text{Leu}}$ , and  $\phi_{\text{Gly}}$  in melanostatin. The family of allowed structures determined from the solid-state NMR data are in excellent agreement with the X-ray structure of the tripeptide. An important feature in the use of REDOR NMR spectroscopy to determine molecular structure is the method's great accuracy in measuring  $^{13}\text{C}$ – $^{15}\text{N}$  distances. Such accuracy is achieved because the observed REDOR effect depends in a straightforward manner on the heteronuclear dipolar coupling constant. The  $r_{\text{CN}}^{-3}$  dependence of  $D_{\text{CN}}$  permits carbon–nitrogen distances of up to 5 Å to be accurately measured. Although the work described here was for a small molecule, the power of the REDOR method is its ability to characterize macromolecules and small molecule/macromolecule complexes (e.g., proteins, inhibitor/enzyme complexes) without limitations imposed by either molecular weight or the need for single crystals. The development of this approach to study such macromolecular systems is currently in progress.

**Acknowledgment.** The authors thank Professors J. Schaefer and T. Gullion for helpful discussions and S. Krimm for suggesting the study of melanostatin. We thank Drs. H.-S. Shieh and M. Chiang for their help in performing the X-ray analysis, and J. Kotyk and W. Hutton for their helpful comments in the prepara-

tion of this manuscript. We gratefully acknowledge the staff of the Mass Spectrometry Lab of the Physical Sciences Center, Monsanto Company.

### Appendix

As discussed in the main text, corrections for the effects of natural-abundance spins must be applied to experimentally measured  $\Delta S/S_0$  values before  $r_{\text{CN}}$  can be accurately determined. This Appendix describes the corrections which were applied to the REDOR data for each of the melanostatin samples.

**Pro-[1- $^{13}\text{C}, ^{15}\text{N}$ ]Leu-Gly-NH<sub>2</sub>.** For Pro-[1- $^{13}\text{C}, ^{15}\text{N}$ ]Leu-Gly-NH<sub>2</sub>, two natural-abundance contributions to  $\Delta S/S_0$  must be considered: (i) natural-abundance [1- $^{13}\text{C}$ ]proline in the peptide bond with labeled [ $^{15}\text{N}$ ]Leu and (ii) labeled [1- $^{13}\text{C}$ ]Leu in the peptide bond with natural-abundance [ $\alpha$ - $^{15}\text{N}$ ]glycine. The [C=O]Pro to [ $\alpha$ -N]Leu and [C=O]Leu to [ $\alpha$ -N]Gly directly-bonded distances are 1.33 Å each. For  $N_{\text{C}} = 16$ ,  $\Delta S/S$  for carbon–nitrogen pairs separated by 1.33 Å is 0.99. We can therefore calculate the natural-abundance corrections to  $\Delta S/S_0$  for this sample by summing the natural-abundance levels of [1- $^{13}\text{C}$ ]Pro (0.011) and [ $\alpha$ - $^{15}\text{N}$ ]Gly (0.0033) and multiplying by 0.99. The total correction of 0.014 was subtracted from the experimentally measured value for  $\Delta S/S_0$  (0.791) before  $D_{\text{CN}}$  was computed.

**[1- $^{13}\text{C}$ ]Pro-Leu-[ $^{15}\text{N}$ ]Gly-NH<sub>2</sub>.** In [1- $^{13}\text{C}$ ]Pro-Leu-[ $^{15}\text{N}$ ]Gly-NH<sub>2</sub>, major natural-abundance contributions to  $\Delta S/S_0$  arise from four fixed-distance sources: (i) labeled [ $\alpha$ - $^{15}\text{N}$ ]Gly to natural-abundance [1- $^{13}\text{C}$ ]Leu, (ii) labeled [1- $^{13}\text{C}$ ]Pro to natural-abundance [ $^{15}\text{N}$ ]Leu, (iii) labeled [ $\alpha$ - $^{15}\text{N}$ ]Gly to natural-abundance [1- $^{13}\text{C}$ ]Gly, and (iv) labeled [1- $^{13}\text{C}$ ]Pro to natural-abundance [ $^{15}\text{N}$ ]Pro. Terms i and ii describe directly-bonded 1.33-Å distances, while terms iii and iv describe two-bond, 2.42 Å-fixed distances. For  $N_{\text{C}} = 32$ ,  $(\Delta S/S)_{1.33\text{Å}} = 1.00$ ;  $(\Delta S/S)_{2.42\text{Å}} = 0.95$ . The required correction is the sum of the natural-abundance levels of [1- $^{13}\text{C}$ ]Leu (0.011) and [ $^{15}\text{N}$ ]Leu (0.0033) multiplied by 1.00 plus the natural-abundance levels of [1- $^{13}\text{C}$ ]Gly (0.011) and [ $^{15}\text{N}$ ]Pro (0.0033) multiplied by 0.95. The total correction of 0.028 was subtracted from the experimentally measured value for  $\Delta S/S_0$  (0.374) before  $D_{\text{CN}}$  was computed.

**Pro-[ $^{15}\text{N}$ ]Leu-[1- $^{13}\text{C}$ ]Gly-NH<sub>2</sub> and Pro-[ $^{15}\text{N}$ ]Leu-[2- $^{13}\text{C}$ ]Gly-NH<sub>2</sub>.** The REDOR data from these two samples were analyzed using a *double-difference* method, as shown in the spectra of Figure 3. Although this procedure eliminates completely the contributions of natural-abundance carbons to  $\Delta S/S_0$ , the measured  $\Delta S/S_0$  values still include contributions from natural-abundance  $^{15}\text{N}$  spins that are near the labeled carbon sites. Experimentally, these latter contributions could be measured using a pair of  $^{13}\text{C}$ -enriched *only* samples. However, the contributions to  $\Delta S/S_0$  from natural-abundance  $^{15}\text{N}$  spins again arise from known, fixed distances (1.33 Å and 2.42 Å) and can be calculated as above. For each sample, these corrections include contributions from natural-abundance levels of both [ $\alpha$ - $^{15}\text{N}$ ]Gly and [carboxamide- $^{15}\text{N}$ ]Gly (0.0033 each). The resulting total, 0.006 (=0.0033 × (1.00 + 0.95)), was subtracted from each of the experimentally determined  $\Delta S/S_0$  values (0.080 for the [1- $^{13}\text{C}$ ]Gly sample; 0.088 for the [2- $^{13}\text{C}$ ]Gly sample) before  $D_{\text{CN}}$  were calculated.

**Registry No.** Pro-Leu-Gly-NH<sub>2</sub>, 2002-44-0; Pro-[1- $^{13}\text{C}, ^{15}\text{N}$ ]Leu-Gly-NH<sub>2</sub>, 144793-06-6; [1- $^{13}\text{C}$ ]Pro-Leu-[ $^{15}\text{N}$ ]Gly-NH<sub>2</sub>, 144793-07-7; Pro-[ $^{15}\text{N}$ ]Leu-[2- $^{13}\text{C}$ ]Gly-NH<sub>2</sub>, 144793-08-8; Pro-[ $^{15}\text{N}$ ]Leu-[1- $^{13}\text{C}$ ]Gly-NH<sub>2</sub>, 144793-09-9.